Earthquake Engineering, Tenth World Conference © 1992 Balkema, Rotterdam. ISBN 90 5410 060 5

The effect of interventions in the floor structural system on the seismic resistance of historic stone-masonry buildings: An experimental study

M.Tomaževič, T.Velechovsky & P.Weiss
Institute for Testing and Research in Materials and Structures, Ljubljana, Slovenia

ABSTRACT: The effect of interventions in the floor structural system on the seismic behaviour of historic stone-masonry buildings has been experimentally investigated. Three two-storey stone-masonry building models have been tested by subjecting them to simulated earthquake ground motion on a simple earthquake simulator. The first model had wooden floors with freely supported joists without tie-beams at floor levels. In the second case, the walls have been tied at floor levels with steel ties, placed on both sides of the walls, whereas wooden floors have been replaced with massive reinforced-concrete slabs and tie-beams in the third case. The influence of the type of connection of walls and floor diaphragm action on the seismic behaviour of the tested type of buildings has been evident.

1 INTRODUCTION

Besides the quality of masonry materials, rigid horizontal floor diaphragm action represents the most important parameter of the seismic resistance of historical urban masonry buildings. It is obvious that, in structural sense, the massive r.c. slabs represent the best possible solution. However, since the replacement of wooden floors is expensive and time consuming intervention in the existing structural system of the building, which is many times also not allowed by conservators of historical monuments, other technological solutions, such as tying the walls with steel ties and making the existing floors more rigid, are applied.

In order to quantify the effects of typical interventions, used in the current renewal practice, on the seismic resistance of historical urban masonry buildings, three models of simple two-storey stone-masonry houses have been tested at the Institute for Testing and Research in Materials and Structures in Ljubljana, Slovenia. The first model had wooden floors with freely supported joists without tie-beams at floor levels. In the second case, the walls have been tied at floor levels with steel ties, placed on both sides of the walls, whereas wooden floors have been replaced with massive reinforced-concrete slabs and tie-beams in the third case. The experiments and the results of tests will be discussed in this paper.

2 CONSTRUCTION OF THE MODELS AND TESTING PROCEDURE

The basic characteristics of old urban stone-masonry houses are as follows: generally, their height does not exceed three to four storeys, with storey height limited to 3 m and the distance between the structural walls, which are at least 50 cm thick, to 4 m. The floors are usually wooden. Sometimes, especially above the ground floor and corridors, the wooden floors are replaced by brick vaults. Only seldom the walls are systematically connected with iron ties at floor levels.

By taking into account the capacity of seismic simulator, the decision was made to build and test the models at 1:4 reduced size scale. The mixture of locally available stone (micaceous quartz sandstone, limestone, tuffs and conglomerate) crushed into adequately sized pieces (6 - 8 cm in diameter) and lime mortar with small quantity of Portland cement added in order to accelerate the attainment of strength, has been used for the construction of the models. The mechanical characteristics of model masonry have been also reduced at 1:4 scale (Table 1).

Only part of the prototype building with simplified, symmetric and idealized characteristics in plan and elevation, has been modelled. However, the main structural characteristics of the prototype building have been respected, such as typical distance between the structural walls, typical storey height, and typical size and position of window and door openings. The structural layout of all models was

Table 1. Mechanical properties of model and prototype masonry materials

	Model	Prototype
Compressive strength f_c (MPa)	0.18	0.90
Shear strength f_t (MPa)	0.03	0.15
Modulus of elasticity E (MPa)	1160	1000
Shear modulus G (MPa)	76	90

identical (Fig.1): the load-bearing walls were oriented in the direction of the shaking-table motion, whereas the walls with the window and door openings were orthogonal to it.

Model A had wooden floors (Fig. 2a): the timber joists, size-reduced according to the geometry scale, have been freely supported by longitudinal walls standing in the direction of the shaking-table motion. Reduced-size planks have been nailed to the joists before the positioning of the floor structure on the walls. In the case of Model A, wooden lintel-beams supported the masonry above the door and window openings. Model B had reinforced-concrete slabs with perimetral bond-beams to help tying the walls at floor levels (Fig. 2b). The slabs have been cast of micro-concrete and reinforced with fully annealed wire, commercially available on the market. Model C was exactly the same as Model A. However, its walls have been tied at floor levels with steel ties (3.8 mm diameter annealed wire has been used), placed at both sides of the walls and anchored with nuts on steel plates at the corners of the walls (Fig. 2c). Before the tests, steel ties have been slightly prestressed (500 μ-strain resulted into the prestressing force 1.19 kN in each bar) in order to active the ties from the very beginning of tests.

In order to achieve the similarity in the distribution of masses along the height of the models, lead bricks (80 kg at each floor level) have been fixed to the floors. By doing this, the level of compressive stresses in the load-bearing walls, required by the laws of the model similarity, has been also automatically fulfilled.

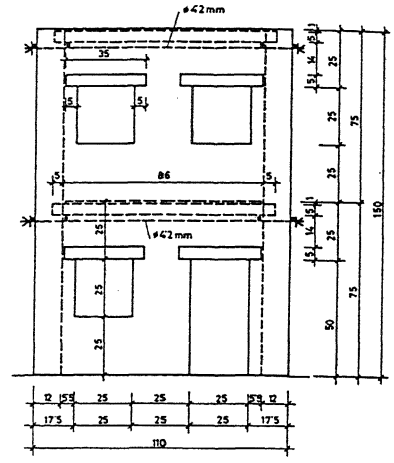

Figure 1. Configuration and dimensions of the tested models

The models were instrumented with accelerometers and displacement meters (LVDT-s) to measure the absolute accelerations and relative displacements of the models in the direction of the seismic motion, respectively. Three instruments of each type, placed at both corners and at mid-span of floor diaphragms, have been fixed to the models at each floor level (Fig.3). In the case of Model C with steel ties, changes in strains in the bars placed along the walls in the direction of seismic motion have been measured with strain-gauges. All measured quantities have been registered in a digital form and stored on a computer disk.

The first 24 seconds of the ground acceleration record of the Montenegro earthquake of April 15, 1979 (N-S component of the Petrovac record) with peak ground acceleration of 0.43 g have been used to simulate the earthquake loads. However, the original record has been modified in order to obtain greater amplification in the range of the expected natural

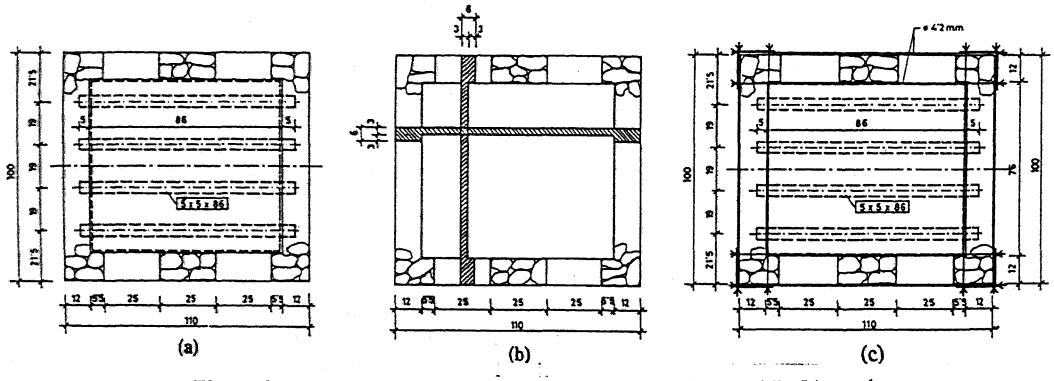

Figure 2. Wooden floor of Model A (a), r.c. slab of Model B (b), and position of steel ties at floor levels of Model C (c)

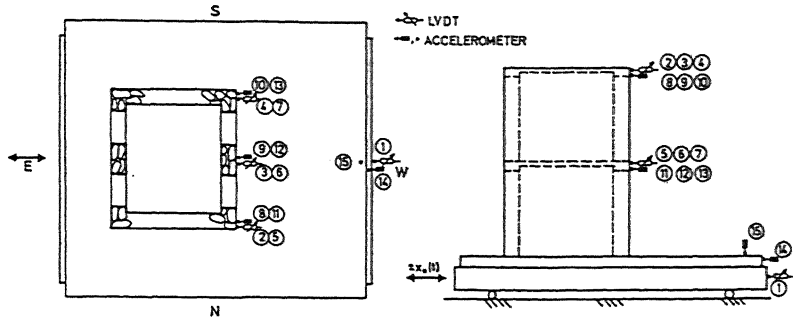

Figure 3. Instrumentation of the models

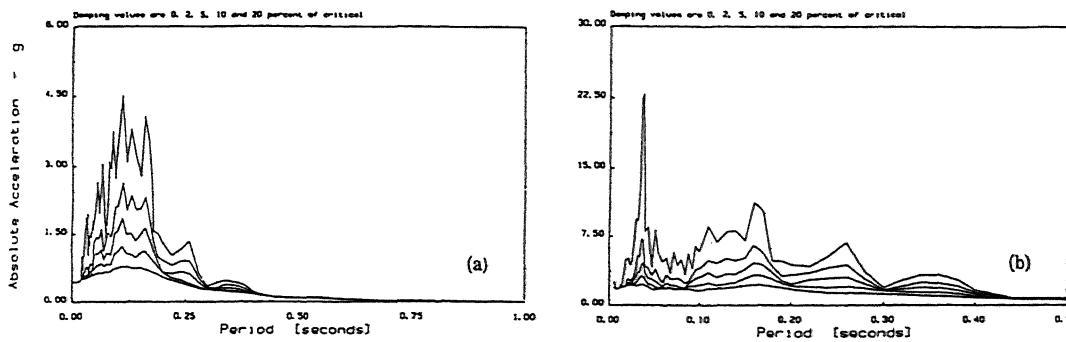

Figure 4. Absolute acceleration response spectra of the prototype earthquake (a) and typical output shaking-table motion during the vibration of one of the models at ultimate state (b)

Table 2. Characteristics of shaking-table motion during the tests of stone-masonry building models

	Design. of test run	Max. sh. table acceleration (g)	Max. top acceleration (g)
Model A	R25	0.12	0.19
	R50	0.35	0.49
	R75	0.50	0.62
	R100	0.74	1.38
	R150	1.33	2.27
	R200	1.41	1.64
Model B	R25	0.16	0.21
	R50	0.40	0.54
	R75	0.77	0.47
	R100	1.08	1.40
	R150	1.74	1.96
	R200	1.81	1.59
Model C	R25	0.19	0.29
	R50	0.36	0.53
	R75	0.92	0.74
	R100	1.01	1.28
	R150	1.97	3.18
	R200	2.23	2.31

frequencies of the models by compressing the duration of the original earthquake by 2-times. As an indication of type of seismic excitation used in the experiments, absolute acceleration response spectra of the input earthquake are compared to the typical spectra of the shaking-table motion at ultimate state of the behaviour of the models in Fig. 4.

The testing procedure was similar during all phases of testing: the models were first subjected to seismic excitation (see Table 2 for information about the testing sequences). Then, by exciting the free vibration of the model, the first natural frequency and the coefficient of the equivalent viscous damping have been determined. For that purpose, each model was hit with a plastic hammer at the second floor level (at the middle of the slab in the case of Model B, at both corners in the case of Models A and C). Fourier analysis has been used to analyze the free vibration response of the models. Finally, the models have been carefully inspected and the damage to models' walls identified and photographed. The behaviour of all models subjected to simulated seismic ground motion has been also recorded with a SVHS video camera.

In all cases, the instruments have been removed from the models after they have suffered substantial damage (test runs designated R200). However, the shaking tests have not been terminated at that point.

3 TEST RESULTS

3.1 *Damage propagation and failure mechanism*

Model A. Although cracks in the walls have been observed already in the initial phases of testing, the model was not seriously damaged until subjected to shaking-table motion of the test run no. R150. Crushing of walls was observed at the bottom corners, and the diagonal cracks in the load-bearing wall at one side of the model propagated almost to the top. An additional crack, oriented in the opposite diagonal direction, developed in the same wall. Vertical cracks at the vertical borders of openings have been observed along the whole height of the model. The width of those cracks increased from bottom to top. During the same testing phase, the first serious signs of separation of walls at the corners of the model have been noticed. The dislocations of the wooden lintel-beams increased. As the most obvious sign of lack of the rigid connection of the walls at floor levels, on of the upper corners of the model disconnected and teared apart.

The increased intensity of motion during the test run no. R200 accelerated the falling apart of the model. All cracks opened and at some locations, stones began to fall off the walls. During the oscillations at large amplitudes the walls separated into several parts so that, after the shaking, the width of some cracks and the dislocations between the separate parts exceeded the value of several millimeters. Model A which partially collapsed during the subsequent test run with the intensity of 250 % of PGA of the prototype input earthquake ground motion, completely collapsed during the repeated shaking of the same intensity.

Model B. Unlike Model A, Model B behaved monolithically up until test run no. R150. A very clear rocking motion of the model was observed up until the most severe phases of shaking. The first serious damage to Model B was observed during the test run no. R150, when the corners of the walls at the foundation slab started crushing because of the intense rocking motion of the model and, consequently, alternating compression and tension at those zones. The window piers in the first storey teared apart. However, although the damage was obviously severe when watching the model to vibrate, the cracks closed and almost disappeared after shaking.

The first visible damage to window piers took place during the test run no. R200, the intensity of which has also increased the amount of damage (crushing) to corner walls. The rocking motion of the model still prevailed, which resulted into the separation between the transversal and longitudinal walls as well as into increase of damage to window piers at the first floor level. The increased intensity of motion during the test run no.R250, when the instruments have been already removed from the model, caused both, tearing apart of the corner parts of the load-bearing walls at the ground level and the disintegration of the window piers of both perforated walls at the ground floor level. The first excitation with 300 % of nominal intensity caused the collapse of the corner parts of the wall on the southern side of the model, the repeated shaking with the same intensity, however, caused the total collapse of the model. In the case of Model B, only the walls in the first storey collapsed. The part of the model above the first floor slab remained virtually undamaged: the second floor simply settled on the debris of the first floor.

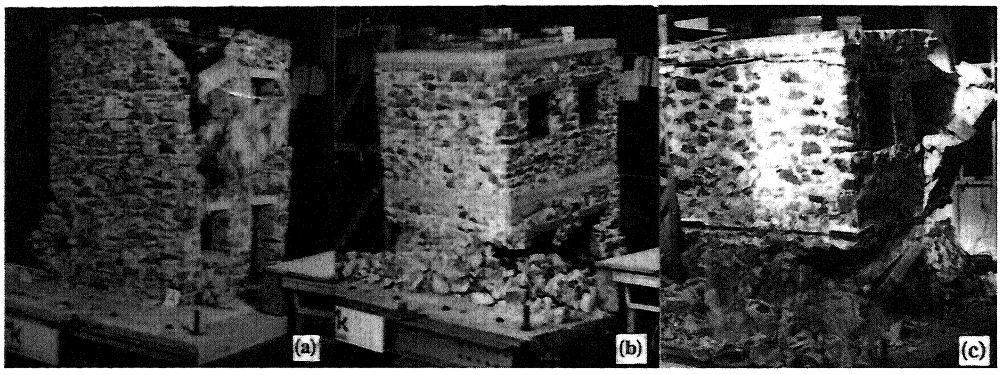

Figure 5. Mechanism of collapse of Model A (a), Model B (b), and Model C (c)

Model C. In a way, the behaviour of Model C was quite similar to the behaviour of Model B. Rocking motion prevailed in the initial phases of test. Tiny cracks in the walls pierced with openings, starting diagonally from the corners of windows and doors, and some cracks at the vertical joints of the walls, have been observed in both storeys during the test run no.R100. However, the cracks in the walls did not pass the tied part of the wall at first floor level. Crushing of corners of the walls at the foundation

slab and opening of cracks in the walls with openings was observed during the test run no.R150. During the same test run, thin diagonal cracks in the load - bearing walls of the first storey in the direction of seismic motion have been observed for the first time.

When subjected to increased intensity of motion during test run no.R200, the shear cracks in the load-bearing walls in the first storey widely opened, and crushing of corners, separation and dislocation of corner parts and window piers took place just below the steel ties at the first floor level. However, no significant damage to the walls of the second storey has been observed. Most instruments have been removed off the model at this time. During the consequent test run no.R250, the load-bearing walls in the first storey partially collapsed. The model remained staying supported by the middle portion of the load-bearing walls and window piers. Although the heavy damage to the walls in the first storey caused evident settlements of parts of the walls just below the first floor level, only separation of the walls and minor dislocations of the corner parts of the walls took place in the second storey. The mechanism of action of steel ties was evident also during the collapse of the model: although parts of the walls started falling off the model also in the second storey, the belts of the masonry around the wooden floors, tied with the steel ties at both floor levels, remained solid until they touched the foundation slab.

The mechanism of collapse of all tested models is shown in Fig.5.

3.2 *Dynamic response and seismic resistance*

The shape of distribution of displacements along the top floor during the characteristic phases of testing (test runs no. R75 to R200) is presented in Fig. 6. In the diagrams, the differences in the behaviour of the tested models, as a consequence of different rigidities of floors and connections of walls, can be clearly noticed. Whereas in the cases of Models B and C the displacement and acceleration amplitudes at the middle of the r.c. slab and at the corners were almost equal during all testing phases, the vibration of the different parts of Model A was not uniform. Looking at the diagram, the effect of tying the walls with steel ties on the seismic behaviour of the buildings can be clearly seen.

In order to obtain information on equivalent viscous damping, the free vibration records, excited by hitting the top part of the models with plastic hammer, have been analyzed. By using the half-power bandwidth method, the values of coefficient of equivalent viscous damping have been evaluated from Fourier amplitude spectra of the free vibration response. The values are between 3 and 6 % of critical damping at the beginning of tests, and are approaching 8 % of critical damping during the strong shaking.

As an indication of the seismic resistance of the tested model buildings, base shear - first storey drift hysteresis envelopes, evaluated from the measured acceleration and displacement response of the models during the individual testing phases, are presented in Fig. 7. In the evaluation of the diagrams in Fig.7 in the non-linear range of vibration, the values of the effective accelerations measured at maximum displacement amplitudes at each storey level, have been taken into account. Much higher, but obviously not realistic values of the base shear result from the peak (maximum) values of the measured acceleration response. As can be seen in Fig.7, practically no difference in the lateral load-bearing capacity can be observed. However, significant difference can be seen as regards the deformability capacity of the tested models: the models with rigid r.c. slabs and wooden floors, but tied walls at the same time (Models B and C, respectively) exhibited much larger deformations before collapse than the model with simply supported wooden floors (Model A).

4 CONCLUSIONS

On the basis of the acceleration and displacement response records obtained during the tests, the differences in the behaviour between the two models have been evaluated. Although the observed behaviour and failure mechanisms significantly differ in the three cases, the differences in the diagrams, which show the relationships between the base shear and first storey drift are not substantial (Fig.11). It can be seen, however, that the available deformability of walls has been fully utilized in the case of the model with rigid slabs (Model B) and wooden floors, but tied walls (Model C), whereas the disintegration of walls decreased the deformability capacity of Model A.

In order to prevent the separation of walls at their intersections, the prestressing of steel ties is recommended (in these experiments, the ties have been prestressed up to about 500 μstrain). In the case

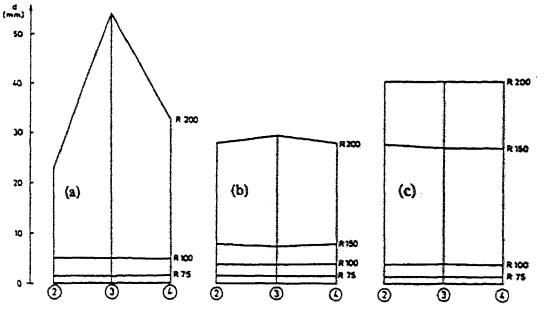

Figure 6. Distribution of displacements along the top floor of Model A (a), Model B (b) and Model C (c) at maximum amplitudes of vibration

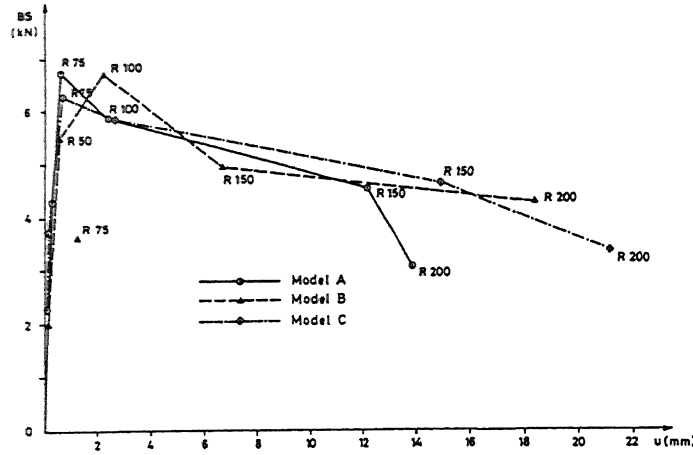

Figure 7. Base shear - first storey drift hysteresis envelopes

of Model C, the increase in strain in the order of only 200 μstrain has been measured during the vibration of the model at ultimate state. The measurements have shown that reinforcing steel bars with 16 mm diameter, which are most frequently used in the current renewal practice, will be enough for efficient tying of the walls in most practical cases.

Table 3. Seismic resistance of prototype buildings

Description of state	Max.ground accel. (g)	Max. base shear coeff.	Dynamic amplif. factor
	Building A		
Initial state	0.12	0.11	1.58
Diagonal cracks, separation of walls	0.74	0.42	1.86
Dislocation of corners disintegration of walls	1.33	0.32	1.71
	Building B		
Initial state	0.16	0.13	1.31
Minor damage to corners	1.08	0.44	1.29
Damage to window piers	1.74	0.32	1.13
Heavy damage to corners and window piers	1.81	0.28	0.88
	Building C		
Initial state	0.19	0.16	1.53
Minor damage to corners	1.01	0.41	1.27
Damage to window piers, cracks in the walls	1.97	0.33	1.61
Crushing of corners, widening of shear cracks	2.23	0.24	1.04

In Table 3, the predicted parameters of the seismic resistance of the prototype buildings of the tested types are presented in correlation to the intensity of the seismic ground motion, expressed in terms of the peak ground accelerations (in g; $g=9.81$ ms^{-2}).

As can be seen, the obtained values of the parameters of the seismic resistance are relatively high. According to the test results, the buildings of both tested types can withstand even the strongest expected earthquake in a relatively good shape. It should be taken into account, however, that the tested models represented houses of relatively good quality stone-masonry walls. As already mentioned, the quality of the existing stone-masonry walls varies in a wide range of values (for example, the values of the tensile strength might vary from 0.02 to 0.15 MPa). Taking this into consideration, it can be seen that the values of the seismic resistance, given in Table 3, should be reduced by up to 2-times in the case of the poor quality stone-masonry buildings of the same height. If such were the case, heavy damage of buildings with wooden floors should be expected during the earthquakes of moderate intensity.

ACKNOWLEDGEMENTS

The research discussed in this article is part of a multi-year project, financed by the Ministry Of Science and Technology of Slovenia and Municipality of the City of Ljubljana. The financial support of both organisations is gratefully acknowledged.